

Hydration Forces Underlie the Exclusion of Salts and of Neutral Polar Solutes from Hydroxypropylcellulose

John Chik,[†] Shimon Mizrahi,[‡] Sulene Chi,[§] V. Adrian Parsegian, and Donald C. Rau*

Laboratory of Physical and Structural Biology, National Institute of Child Health and Human Development, National Institutes of Health, Bethesda, Maryland 20892-0924

Received: July 7, 2004; In Final Form: March 4, 2005

The distance dependence for the preferential exclusion of several salts and neutral solutes from hydroxypropyl cellulose (HPC) has been measured via the effect of these small molecules on the thermodynamic forces between HPC polymers in ordered arrays. The concentration of salts and neutral solutes decreases exponentially as the spacing between apposing nonpolar HPC surfaces decreases. For all solutes, the spatial decay lengths of this exclusion are remarkably similar to those observed between many macromolecules at close spacings where intermolecular forces have been ascribed to the energetics of water structuring. Exclusion magnitudes depend strongly on the nature and size of the particular salt or solute; for the three potassium salts studied, exclusion follows the anionic Hofmeister series. The change in the number of excess waters associated with HPC polymers is independent of solute concentration suggesting that the dominating interactions are between solutes and the hydrated polymer. These findings further confirm the importance of solvation interactions and reveal an unexpected unity of Hofmeister effects, preferential hydration, and hydration forces.

Introduction

A vast, well-reviewed literature^{1–8} describes the preferential interactions of salts and neutral solutes with proteins, nucleic acids, and other macromolecules. The partial exclusion of small molecules from surfaces can have energetic consequences as important as their direct binding for stabilizing compact, native conformations, enhancing ligand binding, and strengthening macromolecular association and assembly reactions. The ability of salts to precipitate or solubilize proteins was first systematized by Hofmeister resulting in his classical ordering of anions and cations.⁹ Changes in local water structuring have long been thought to underlie Hofmeister interactions.^{1,9–11} Two general mechanisms have been proposed to account for exclusion of neutral osmolytes from exposed surfaces. “Crowding”^{12,13} is based on a steric exclusion, dependent only on solute size and shape but not chemical nature. Alternatively, the interaction of macromolecule and solute with water can be more favorable than direct solute-surface interactions also resulting in a “preferential hydration”.^{7,14} In this case, the chemical nature of the solute is additionally important. The large literature on exclusion of small (MW < ~500) solutes from proteins and nucleic acids^{1,3–6,8,15} indicates that exclusion depends not only on size but also the chemical nature of the solute. Despite the abundance of preferential hydration data, however, there is no clear indication of the physical nature of the repulsive interactions between solutes and macromolecular surfaces.

The spatial distribution of solute or salt concentration from the surface will be determined by the nature of the forces underlying exclusion. We have previously reported the distance dependence of forces between macromolecules in condensed arrays for many diverse systems.^{16–21} Forces can be measured using osmotic stress coupled with X-ray diffraction. Condensed arrays of ordered macromolecules are equilibrated against aqueous solutions of typically poly(ethylene glycol) (PEG) that is excluded from the condensed phase and applies an osmotic pressure on it. Water and small solutes are free to exchange and equilibrate between the PEG solution and the macromolecular phase. Distances between macromolecules as a function of PEG osmotic pressure are determined from Bragg scattering of X-rays. These are measurements of thermodynamic forces since configurational fluctuations can contribute. A loss of configurational entropy as macromolecules approach can be due either to simple steric interactions as observed for guar and its derivatives²² or to confining intermolecular forces as observed for DNA, for example, at low osmotic pressures.^{23,24} At close distances (the last 10–15 Å separation) and high pressures, force curves observed are strikingly similar for a wide variety of charged and uncharged polymers. Forces vary exponentially with a 3–4 Å decay length. Force magnitudes are quite sensitive to the nature of the macromolecular surface. Because of the similarity of these forces and their contrast from commonly expected forces and since these forces for uncharged macromolecules have been measured in distilled water, we have postulated that water structuring or hydration forces dominate the interactions between surfaces at close distances.^{17,21}

Any preferential interaction of salts and neutral solutes with macromolecules in the condensed phase must necessarily alter thermodynamic force curves of the macromolecules. Here we examine such interactions of several salts and polar solutes with the neutral polymer hydroxypropyl cellulose (HPC) building on our previous measurements of HPC forces in distilled water.¹⁸ Since HPC is uncharged, we can focus on solvation and avoid

* Corresponding author: Laboratory of Physical and Structural Biology, NICHD, National Institutes of Health, Building 9, Rm 1E114, Bethesda, MD 20892. Telephone: (301)-402-4698. Fax: (301)-402-9462. E-mail: raud@mail.nih.gov.

[†] Present address: Department of Biochemistry and Molecular Biology, Faculty of Medicine, University of Calgary, Calgary, Alta., Canada T2N 4N1.

[‡] Present address: Department of Food Engineering and Biotechnology, Technion-Israel Institute of Technology, Haifa 32000, Israel.

[§] Present address: School of Medicine, Duke University, Durham, NC 27710.

salt interactions due to charge neutralization. Specifically, from the sensitivity of HPC force curves to solute or salt concentration, we can extract changes in numbers of water molecules and solutes or salts associated with the HPC phase as the distance between macromolecular surfaces varies using a Maxwell relation built on the Gibbs–Duhem equation.

We find that this hydrophobically modified cellulose derivative strongly excludes salts (KF, KCl, NaCl, and KBr) and polar osmolytes (betaine glycine, glycerol, and α -methyl glucoside) but that the nonpolar solute 2-methylpentane-(2,4)-diol (MPD) is not observably included or excluded. The exclusion of salts and polar solutes varies approximately exponentially with the distance between HPC polymers with decay lengths varying between ~ 3 and 4.5 Å. The magnitude of exclusion depends on the nature of the salt or solute. Among anions, exclusion follows the Hofmeister series, $F^- > Cl^- > Br^-$.

The change in the number of excess waters as the spacing between HPC polymers changes is independent of solute or salt concentration. By integrating over distance, we can estimate a total number of preferentially included waters. At 20°C , the number of excess waters associated with the most highly excluded salt KF is equivalent to a bit more than the first hydration layer. Glycerol and KBr are 3–4-fold less excluded.

We can independently infer exclusion from the temperature-favored precipitation of HPC from dilute solution. The transition temperature decreases with increasing concentration of excluded solutes or salts. The change in preferential hydration accompanying precipitation of HPC extracted from the observed temperature dependence is in good agreement with the integrated number of waters extracted from the changes in forces with added salts or neutral solutes.

The magnitude of the number of excess waters and the dependence on the nature of the salt or solute, but not on concentration, are characteristic of many solute exclusion or preferential hydration measurements. The common 3–4 Å decay length of the exponentially varying exclusion for all the salts and solutes indicates that these small molecules interact with the HPC surface through water structuring or hydration forces. This remarkable convergence of Hofmeister interactions, osmolyte exclusion and preferential hydration, and hydration forces offers new opportunities to think about salting-in and salting-out and about the action of small solutes on macromolecular stability and interactions.

Methods and Materials

Materials. Hydroxypropylcellulose (HPC) was purchased from Polysciences, Inc., and used without further purification. The polymer had an average molecular weight of 60 000 and ~ 3 hydroxypropyl groups incorporated/glucose monomer. Poly(ethylene glycol) (MW 8000, microselect grade), betaine glycine ($>99\%$), α -methyl glucoside ($>99\%$), and 2-methyl-2,4-pentanediol ($>99\%$) were purchased from Fluka Chemical Company. All salts were analytical grade.

Osmotic Stress. Parsegian et al.¹⁶ describe the method for direct force measurement by osmotic stress. In brief, condensed macromolecular arrays are equilibrated against a bathing polymer solution, typically poly(ethylene glycol), PEG, of known osmotic pressure that is excluded from many condensed macromolecular arrays, including HPC. Water and small solutes are free to exchange between the PEG and condensed HPC phases. At equilibrium, the osmotic pressures in both the polymer and macromolecular phases are the same, as are the chemical potentials of all exchangeable species. If the condensed macromolecular phase is sufficiently ordered, the intermolecular

distance can be determined as a function of the applied PEG stress by Bragg scattering of X-rays.

As described previously,¹⁸ ordered arrays of HPC were prepared by slowly concentrating a 2% solution by dialysis against a 40% PEG (8000 MW) solution using a Pierce Microdialysis System 500 with a 1000 MWCO membrane. The final transparent, solid HPC films had a thickness of ~ 0.5 mm. Small samples ($\sim 1 \times 1$ mm) were cut from the films and used for equilibration and force measurements. HPC pellets were equilibrated against 1 mL solutions of PEG-osmolyte in screw capped Eppendorf tubes for ~ 3 weeks with two changes of solution.

The measured force curves for these salts and solutes are completely reversible. The same interaxial spacing is observed for HPC samples equilibrated directly against osmolyte solution with high PEG osmotic pressures as with samples equilibrated first against osmolyte solution with low PEG concentration and then against the high PEG osmotic pressure, osmolyte solution. Similarly, high PEG pressure samples reequilibrated against osmolyte solutions with low PEG osmotic pressure give the same interaxial spacing as samples initially equilibrated against low PEG osmotic pressure, osmolyte solution.

The preferential exclusion of KCl, KF, α -methyl glucoside, and betaine glycine from the condensed HPC phase was confirmed as described previously.¹⁸ Dry HPC samples (10–15 mg) were hydrated at room temperature with limited amounts of solutions (~ 40 μL) with high enough solute concentrations such that precipitation of HPC occurs at less than 20°C , (1 M KF, 1.8 M KCl, 2.5 *m* betaine glycine, and 3.5 *m* α -methylglucoside). The change in the refractive index of the bathing solution before and after hydration showed that *little* salt or solute ($<10\%$ of the initial bathing solution concentration) is included in the HPC phase. The preferential hydration of HPC in the presence of KBr and glycerol was too weak to measure reliably the exclusion of these two solutes by this technique. The concentrations of glycerol and KBr necessary to maintain a condensed pellet of HPC (>5 *m* and 4 M, respectively) were too high for accurate measurement.

Osmotic pressures of the PEG-solute solutions were measured directly using a Vapro vapor pressure osmometer (model 5520XR, Wescor Corp.). Osmotic pressures were additive over the range of PEG and solute concentrations examined to within $\sim 15\%$ for glycerol, and $\sim 10\%$ for KBr and MPD. There was more nonadditivity (up to $\sim 50\%$ excess osmotic pressure) for KF, KCl, betaine glycine, and α -methyl glucoside in the PEG concentration range examined. Simultaneous measurement of K^+ activities using a K^+ selective solid-state electrode (Thomas Scientific, Inc.) showed, however, that to within 10% the excess osmotic pressure was due to an increased salt activity. We assumed the same behavior for betaine glycine and α -methyl glucoside. Solute and salt osmotic pressures, Π_s , in the presence of PEG were taken as the difference between the measured osmotic pressures of solute-PEG solution and the solution of PEG at the same weight fraction, f_w , but without added solute,

$$\Pi_s = \Pi([\text{solute}], [\text{PEG}] = f_w) - \Pi([\text{solute}] = 0, [\text{PEG}] = f_w) \quad (1)$$

These data are available as Supporting Information.

X-ray Scattering. An Enraf-Nonius Service Corp. (Bohemia, NY) fixed copper anode Diffractis 601 X-ray generator equipped with double focusing mirrors (Charles Supper Co.) was used for X-ray scattering. HPC samples were sealed with a small amount of equilibrating solution in the sample cell, and then

mounted into a temperature-controlled holder at 20 °C. A helium filled Plexiglas cylinder with Mylar windows was between the sample cell and image plate, a distance of ~ 16 cm. Diffraction patterns were recorded by direct exposure of Fujifilm BAS MS image plates and digitized with a Fujifilm BAS 2500 scanner. The images were analyzed using the FIT2D (copyright A. P. Hammersley, ESRF) and SigmaPlot 8.0 (SPSS Inc.) programs. The sample to image plate distance was calibrated using powered *p*-bromobenzoic acid.

Cloud Point Transitions. Cloud point measurements of HPC precipitation from dilute solution were performed as described previously.¹⁸ The turbidity of a 0.1 mg/mL HPC solution was measured at 350 nm with a Perkin-Elmer Lambda 900 spectrophotometer during slow heating and cooling cycles. The temperature was controlled using a programmable Neslab model RTE 111 refrigerated bath/circulator.

Thermodynamics

When the HPC phase is brought to equilibrium with PEG solutions of separately estimated polymer osmotic stress, the PEG pressure can be viewed as acting through a semipermeable membrane separating a pure salt solution from HPC plus salt. The Gibbs–Duhem relation $n_w d\mu_w + n_s d\mu_s = 0$ holds with the pure saltwater phase as it does also in the polymer + salt solution, $N_p d\mu_p + N_w d\mu_w + N_s d\mu_s = 0$. By the transitivity of equilibrium, the HPC too can be considered to be under the pressure of a membrane permeable only to salt and to water.

Visually, the osmotic action of PEG that is excluded from the HPC phase is equivalent to a piston applying a pressure Π_{PEG} through a semipermeable membrane that separates the HPC phase from a reference solution of water and salt or neutral solute that is present in vast excess.^{18,25,26} If the HPC phase contains N_s and N_w molecules of solute and water per HPC unit and the reference phase n_s and n_w molecules, then at constant temperature and hydrostatic pressure the Gibbs–Duhem equations for these phases can be combined to relate changes in HPC chemical potential, $d\mu_{\text{HPC}}$, with changes in PEG osmotic pressure and solute concentration. The Gibbs–Duhem equations for the HPC and reference phases are

$$d\mu_{\text{HPC}} = -N_s d\mu_s - N_w d\mu_w \quad \text{and} \quad n_w d\mu_w^{\text{ref}} = -n_s d\mu_s^{\text{ref}} \quad (2)$$

The osmotic pressure dependence of the distance measured between HPC polymers in the condensed phase without added solutes is the same for 8×10^3 and 2×10^4 average MW PEG as well as for 1×10^4 average MW poly(vinylpyrrolidone) (PVP). From this singular dependence on osmotic pressure, we know that none of these three polymers enters the HPC phase. That is, $n_{\text{PEG}} = 0$ in the HPC phase so there is no $n_{\text{PEG}} d\mu_{\text{PEG}}$ term in the Gibbs–Duhem equation for the HPC-containing bathing solution. Similarly, because little or no change in the size of HPC pellets is observed even with repeated changes into fresh PEG solutions, we know that HPC negligibly enters the PEG phase, i.e., $n_{\text{HPC}} = 0$; we can neglect the $n_{\text{HPC}} d\mu_{\text{HPC}}$ term in the PEG reference solution.

In terms of the reference solution and PEG piston, the chemical potentials of the exchangeable species in the HPC phase are given by

$$d\mu_s = d\mu_s^{\text{ref}} \quad \text{and} \quad d\mu_w = d\mu_w^{\text{ref}} - \bar{v}_w d\Pi_{\text{PEG}} \quad (3)$$

where \bar{v}_w is the volume of a water molecule which we safely assume to be constant at the low pressures used here. Combining these equations, we have either

$$d\mu_{\text{HPC}} = V_w d\Pi_{\text{PEG}} - N_w \left(1 - \frac{(N_s/N_w)}{(n_s/n_w)} \right) d\mu_w^{\text{ref}} = V_w d\Pi_{\text{PEG}} + \bar{v}_w \Gamma_w d\Pi_s \quad (4)$$

or

$$d\mu_{\text{HPC}} = V_w d\Pi_{\text{PEG}} - N_s \left(1 - \frac{n_s/n_w}{N_s/N_w} \right) d\mu_s^{\text{ref}} = V_w d\Pi_{\text{PEG}} - \Gamma_s d\mu_s^{\text{ref}} \quad (5)$$

where $V_w = \bar{v}_w N_w$, and $d\Pi_s = -\bar{v}_w d\mu_w^{\text{ref}}$, the differential solute contribution to the osmotic pressure. $\Gamma_w (= N_w(1 - (N_s/N_w)/(n_s/n_w)))$ and $\Gamma_s (= N_s(1 - (n_s/n_w)/(N_s/N_w)))$ are the excess number of water and solute molecules, respectively, associated with HPC, also termed preferential interaction coefficients. As is readily apparent, the excess water can also be considered a measure of the partition coefficient of solute between the bulk and HPC phases, $(N_s/N_w)/(n_s/n_w)$. Because water and solute activities are necessarily coupled, the data can be analyzed equally validly as either an excluded solute Γ_s coupled to the solute chemical potential or a preferential hydration Γ_w linked to the solute contribution to the osmotic pressure. We focus here on changes in preferential hydration coupled to changes in the solute contribution to the osmotic pressure since we find that $\Delta\Gamma_w$ is independent of solute concentration, unlike the change in excluded salt, $\Delta\Gamma_s$.

At this point, it is helpful to recognize conservation of energy as expressed by a Maxwell cross-relation associated with eq 4

$$\frac{\partial \Gamma_w}{\partial \Pi_{\text{PEG}}} \Big|_{\Pi_s} = \frac{\partial V_w}{\bar{v}_w \partial \Pi_s} \Big|_{\Pi_{\text{PEG}}} \quad (6)$$

Because it is the net change in Γ_w that we seek, we integrate $\Delta\Gamma_w$ while holding Π_s fixed.

$$\Delta\Gamma_w = \int_{\Pi_{\text{PEG},1}}^{\Pi_{\text{PEG},2}} \frac{\partial V_w}{\bar{v}_w \partial \Pi_s} \Big|_{\Pi_{\text{PEG}}} d\Pi_{\text{PEG}} = \int_{V_{w,1}}^{V_{w,2}} \frac{\partial V_w}{\partial \Pi_s} \Big|_{\Pi_{\text{PEG}}} \frac{\partial \Pi_{\text{PEG}}}{\partial V_w} \Big|_{\Pi_s} \frac{dV_w}{\bar{v}_w} = - \int_{V_{w,1}}^{V_{w,2}} \frac{d\Pi_{\text{PEG}}}{d\Pi_s} \Big|_{V_w} \frac{dV_w}{\bar{v}_w} \quad (7)$$

where we recognize that for constant $V_w = V_w(\Pi_{\text{PEG}}, \Pi_s)$,

$$\frac{d\Pi_{\text{PEG}}}{d\Pi_s} \Big|_{V_w} = - \frac{(\partial V_w / \partial \Pi_s) \Big|_{\Pi_{\text{PEG}}}}{(\partial V_w / \partial \Pi_{\text{PEG}}) \Big|_{\Pi_s}} \quad (8)$$

Equation 7 then empirically yields $\Delta\Gamma_w$, the change in the number of excess waters associated with HPC, from the measured change, $d\Pi_{\text{PEG}}/d\Pi_s|_{V_w}$, in PEG pressure necessary to maintain a fixed interaxial spacing or volume while varying Π_s , the salt contribution to the osmotic pressure.

We relate the Bragg spacing, D_{Br} , measured by X-ray scattering to the volume V_w per length L along the HPC backbone by¹⁸

$$dV_w = 2LD_{\text{Br}} dD_{\text{Br}} \quad (9)$$

The effectiveness of solute to change the thermodynamic force curve of HPC depends on the extent of exclusion or partitioning, $(N_s/N_w)/(n_s/n_w)$. If there is no difference in concentration between the two phases, then $\partial \Pi_{\text{PEG}} / \partial \Pi_s|_{V_w} = 0$ and, consequently, $\Delta\Gamma_w = 0$. At the other extreme, if solute is completely excluded from

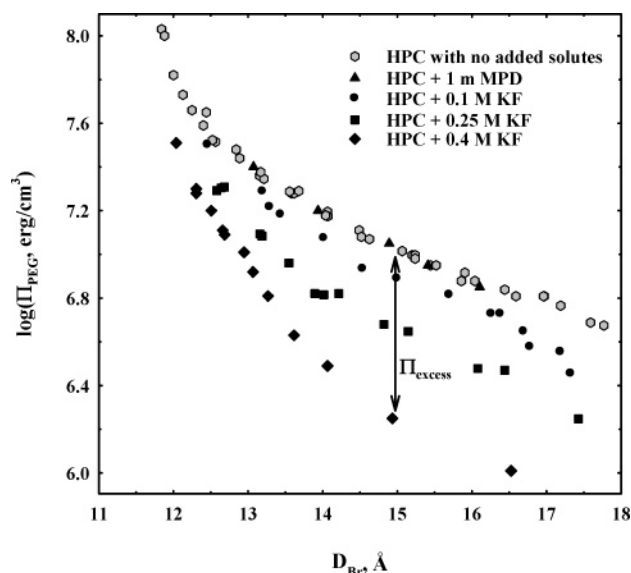


Figure 1. Thermodynamic force curves of HPC change with added KF, but not with MPD. Condensed ordered arrays of HPC were equilibrated at 20 °C against PEG solutions containing various concentrations of MPD and KF. Bragg spacings between HPC polymers were determined by X-ray diffraction as a function of PEG osmotic pressure, Π_{PEG} . The force curves in the absence of any added salt or solute and with 1 m MPD are indistinguishable. There is no preferential interaction of HPC with MPD. In contrast, the Bragg spacing between polymer chains at constant Π_{PEG} decreases significantly as the concentration of KF increases. The arrow illustrates the apparent excess pressure, Π_{excess} , applied by 0.4 M KF at 15 Å.

the HPC phase ($N_s/N_w = 0$), the solute acts identical with PEG, $\partial\Pi_{\text{PEG}}/\partial\Pi_s|_{V_w} = -1$ and $\Delta\Gamma_w = \Delta N_w$.

Results

Figure 1 shows the variation of the HPC interaxial Bragg spacing (D_{Br}) on the PEG osmotic pressure, Π_{PEG} , without added solute, with added 2-methyl-2,4-pentanediol (MPD), and with several KF concentrations at 20 °C. The Bragg spacing for dry HPC is 10.9 Å. In the absence of added salts or solutes, two force regimes are apparent for this range of spacings.¹⁸ There is a short ranged, rapidly changing force at very close spacings (the last 1–2 Å) that is temperature insensitive. This force is likely due to steric repulsions between groups on the HPC surface. At longer spacings the interaction can be characterized as an exponentially varying force with a decay length of ~ 3.5 Å. The amplitude of this force, but not its decay length, is dependent on temperature, decreasing with increasing temperature. The force changes from repulsive to attractive at ~ 40 °C.

MPD has no observable effect on the force curve of HPC and, therefore, from Equations 4 and 5 interacts weakly if at all with HPC. The strong dependence of spacing on KF concentration necessarily means a strong interaction of this salt with HPC and a consequent difference in KF concentrations in the HPC phase and the bathing PEG solution. An exclusion of KF from the HPC phase was confirmed by solvation of dry HPC films with small amounts of KF solution and measurement of an increased salt concentration remaining in the supernatant as described previously for NaCl.¹⁸

Figure 2 shows the decrease in Π_{PEG} necessary to maintain a constant interaxial spacing with increasing Π_{KF} at two distances interpolated from the data in Figure 1. The contribution of KF to the solution osmotic pressure, Π_{KF} , was taken as the difference in osmotic pressures between PEG solutions with

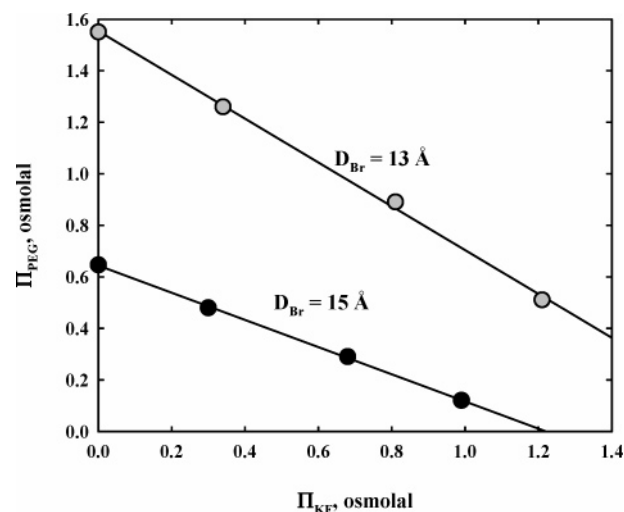


Figure 2. The PEG osmotic pressure necessary to maintain constant D_{Br} (constant volume) depends linearly on the KF contribution to the total osmotic pressure. PEG osmotic pressures as a function of KF concentration are interpolated from forces curves as shown in Figure 1 for two Bragg spacings. The slopes, $(d\Pi_{\text{PEG}}/d\Pi_{\text{KF}})|_{V_w}$, are -0.80 and -0.48 at $D_{\text{Br}} = 13$ and 15 Å, respectively. A slope of -1 is expected for complete exclusion and 0 for no exclusion or inclusion. Linearity indicates that the excess water, $\Delta\Gamma_w$, is independent of KF concentration.

and without added KF (cf. eq 1 and the discussion in Methods and Materials). The linear dependence indicates that $(\partial\Pi_{\text{PEG}}/\partial\Pi_{\text{KF}})|_{V_w}$ is constant and, consequently from eq 7 that $\Delta\Gamma_w$ is also constant, i.e., independent of KF concentration at each spacing. This indicates that the partition coefficient of solute between the bulk solution and HPC phase, $(N_s/N_w)/(n_s/n_w)$, is insensitive to the bulk concentration. The slopes of the lines are -0.80 and -0.48 at $D_{\text{Br}} = 13$ and 15 Å, respectively. These slopes can vary between 0 for no exclusion and -1 for complete exclusion from the HPC phase.

For a linear dependence between Π_{PEG} and Π_{KF} , each measured data point can be converted into a slope. An apparent excess osmotic pressure due to a difference in KF concentrations between the reference and HPC phases (illustrated by the arrow in Figure 1) can be defined as $\Pi_{\text{excess}} = \Pi_{\text{PEG}}(D_{\text{Br}}, \Pi_{\text{KF}} = 0) - \Pi_{\text{PEG}}(D_{\text{Br}}, \Pi_{\text{KF}})$. The slope, $d\Pi_{\text{PEG}}/d\Pi_{\text{KF}}$, at constant D_{Br} is $-\Pi_{\text{excess}}/\Pi_{\text{KF}}$. Figure 3a shows the variation of this parameter for KF with Bragg spacing. The overlap of the data for KF concentrations ranging from 0.1 to 0.8 M confirms the insensitivity of $\Delta\Gamma_w$ to salt concentration seen in Figure 2. Additionally, there is little difference in exclusion between 5 and 20 °C. At close spacings, KF is virtually completely excluded from the HPC phase, $\Pi_{\text{excess}}/\Pi_{\text{KF}} \sim 1$. Four points ranging between 0.72 and 1.1 M KF without any added PEG and spanning a range of Bragg spacings from 12.5 to 16 Å are also included. A concentration of 0.7 M KF is sufficient to maintain a condensed array at 20 °C. The overlap of the KF data with and without PEG indicates that nonideal interactions of PEG and KF have been correctly evaluated. Over this approximate 5-fold change in $\Pi_{\text{excess}}/\Pi_{\text{KF}}$, the data can be adequately described by an exponential with decay length ~ 4.5 Å.

Parts b–f of Figure 3 show analogous plots of $\Pi_{\text{excess}}/\Pi_s$ for KCl, KBr, the zwitterionic solute betaine glycine, and the neutral polyols glycerol and α -methyl glucoside. Data are shown for at least three concentrations and, except for KBr, for 5 and 20 °C. The KCl data are indistinguishable from the NaCl results published previously.¹⁸ As with KF, the overlap of the different concentrations indicates that changes in excess water associated with HPC, $\Delta\Gamma_w$, are independent of solute concentration for all

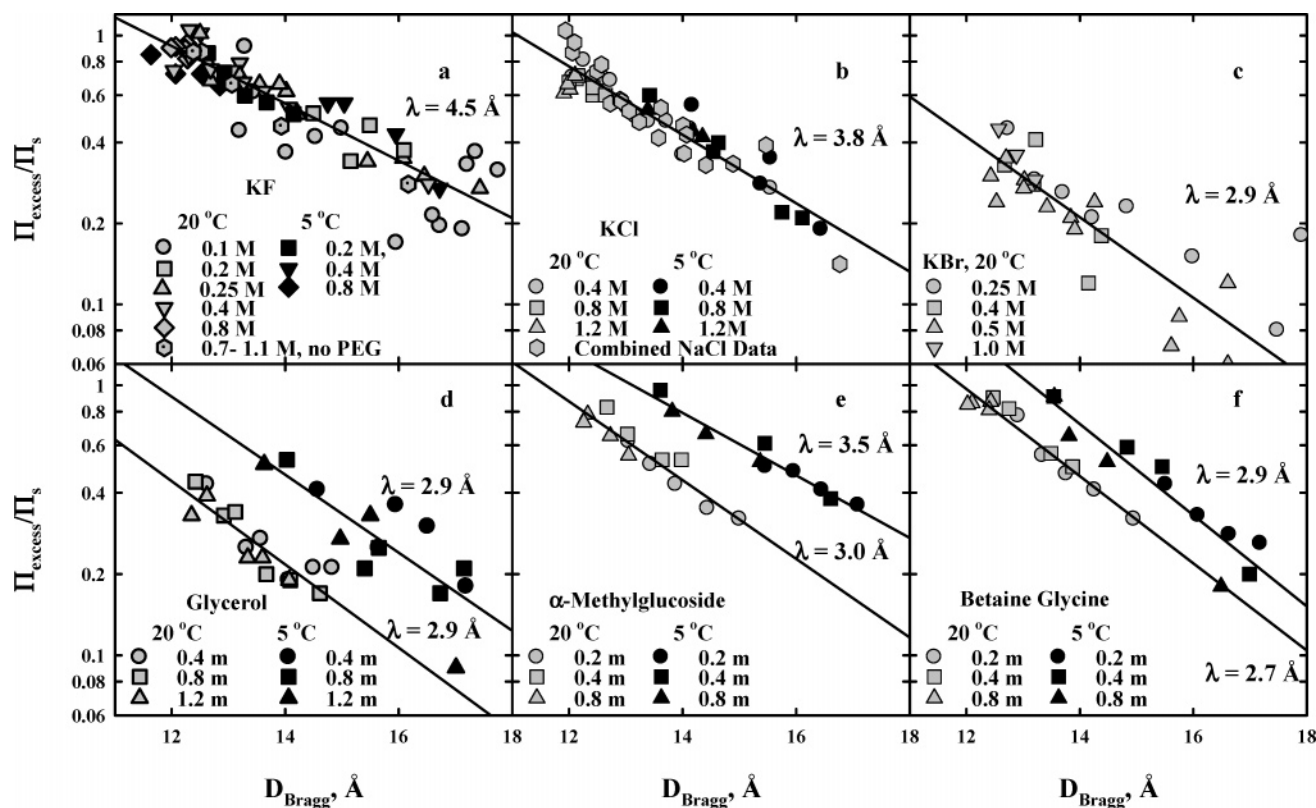


Figure 3. The spatial dependence of the change in the excess water associated with HPC with volume, $d\Delta\Gamma_w/dV = -\Pi_{\text{excess}}/\Pi_s$, is shown for three salts and three neutral solutes: (a) KF; (b) KCl and NaCl; (c) KBr; (d) glycerol; (e) α -methyl glucoside; (f) betaine glycine. Π_{excess} is the difference between the PEG pressure with added solute and the interpolated PEG pressure without solute at the same spacing, as illustrated by the double arrow in Figure 1. Π_s was taken as the difference between the osmotic pressures of PEG with solute and PEG only solutions. The data for all solutes span at least a 3-fold range in concentration and are shown for 5 and 20 °C, except for KBr. The overlap of the data for the different concentrations indicates that $\Delta\Gamma_w$ is independent of solute concentration. Data are also shown in part a for 0.72–1.1 M KF in the absence of PEG. The combined NaCl data in part b is taken from Bonnet-Gonnet et al.¹⁸ Although the magnitude of exclusion is sensitive to the identity of the solute or salt, the spatial dependence is strikingly similar for all. Analyzed as an exponential, the decay length λ varies between 3 and 4.5 Å characteristic of a repulsive hydration force.

TABLE 1: Characterization of Salt and Solute Exclusion from HPC

solute or salt	$\lambda,^a \text{ \AA}$	A^a	$\Delta\Gamma_w^{\text{total}, b}$	$\Delta R,^c \text{ \AA}$	$-(dT_0/d\Pi_s),^d$ °C/osm	
					expt	calcd
KF, 5 and 20 °C	4.5 ± 0.4	1.2 ± 0.2	55	3.6	13.9	15.3
KCl, 5 and 20 °C	3.8 ± 0.2	1.0 ± 0.15	37	2.6	7.6	8.9
NaCl, 20 °C ^e	3.9 ± 0.3	0.95 ± 0.2	37	2.6		
KBr, 20 °C	2.9 ± 0.3	0.6 ± 0.1	16	1.25	3.8	4.0
glycerol, 5 °C	2.9 ± 0.6	1.35 ± 0.5	35	2.5		
glycerol, 20 °C	2.9 ± 0.6	0.65 ± 0.2	17	1.3		
betaine, 5 °C	2.9 ± 0.3	1.9 ± 0.3	45	3.1		
betaine, 20 °C	2.7 ± 0.2	1.45 ± 0.2	34	2.4	7.7	8.4
MeGlucoside, 5 °C	3.5 ± 0.6	2.0 ± 0.3	59	3.8		
MeGlucoside, 20 °C	3.0 ± 0.3	1.25 ± 0.2	34	2.4	6.3	8.3

^a $\frac{\Pi_{\text{excess}}}{\Pi_s}(D_{\text{Br}}) = Ae^{-(D_{\text{Br}}-D_0)/\lambda}$ where D_0 is the “dry” spacing of HPC (10.9 Å). ^b $\Delta\Gamma_w^{\text{total}} = -\int_{D_0}^{\infty} \frac{\partial \Pi_{\text{PEG}}}{\partial \Pi_s} \bigg|_{V_w} \frac{dV_w}{V_w} \approx \int_{D_0}^{\infty} 2L \frac{\Pi_{\text{excess}}}{\bar{V}_w \Pi_s} D_{\text{Br}} dD_{\text{Br}}$ where L is the length along HPC (calculated for 10 Å), and $\Pi_{\text{excess}}/\Pi_s$ is the smaller of 1 and $Ae^{-(D_{\text{Br}}-D_0)/\lambda}$, i.e., the maximal normalized pressure that can be applied by excluded solute is 1. ^c The distance of the equivalent Gibbs dividing surface from the HPC surface, ΔR , was calculated from, $L((D_0 + \Delta R)^2 - D_0^2) = \bar{V}_w \Delta\Gamma_w^{\text{total}}$. ^d Calculated using eq 10 with $\Delta\Gamma_w(\infty \rightarrow 12\text{ \AA}) \approx 2L \int_{\infty}^{12\text{ \AA}} \frac{\partial \Pi_{\text{PEG}}}{\partial \Pi_{\text{salt}}} \bigg|_{V_w} \frac{D_{\text{Br}} dD_{\text{Br}}}{\bar{V}_w} = -\frac{2L}{\bar{V}_w} A\lambda(\lambda + 12\text{ \AA})e^{-1.1/\lambda}$. From our previous measurements, $\Delta S \sim 12 \text{ k}$ for $L = 10 \text{ \AA}$ and $D_{\text{Br}} = 12 \text{ \AA}$. ^e Data taken from Bonnet-Gonnet et al.¹⁸

these compounds within experimental error. Unlike KF and KCl, the neutral solutes all show a substantial difference between 5 and 20 °C. The spatial dependence of exclusion is strikingly similar for all the salts and neutral solutes. The curves can be adequately described by an exponential variation of $\Pi_{\text{excess}}/\Pi_s$ with Bragg spacing. The decay lengths vary between ~ 3 and 4.5 Å. Preexponential factors differ significantly among the

solutes. Amplitudes, A , and decay lengths, λ , are summarized in Table 1.

The change in the number of excess waters associated with an HPC length of 10 Å as a function of spacing can be estimated by integrating eq 7. If we extrapolate the $\Pi_{\text{excess}}/\Pi_s$ to large spacings, then $\Delta\Gamma_w$ also varies exponentially with D_{Br} with about the same decay length. The estimated total numbers of excess

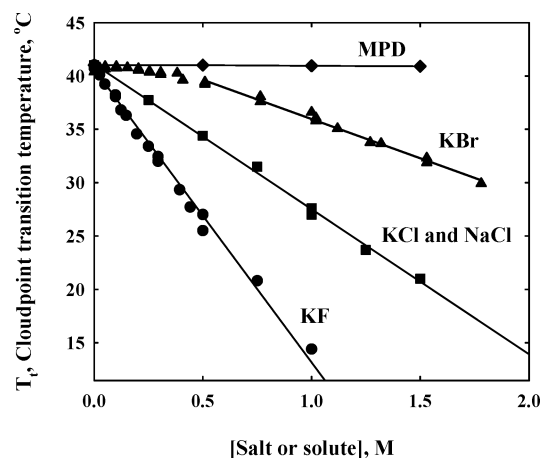


Figure 4. Dependence of the precipitation temperature of HPC in dilute solution (~ 0.1 mg/mL) on salt or solute concentration is shown for MPD, KBr, KCl, NaCl, and KF. The slopes are determined by the entropy change of the transition and $\Delta\Gamma_w$ accompanying assembly. We have previously¹⁸ calculated the entropy change from the temperature dependence of the thermodynamic force and can calculate $\Delta\Gamma_w$ from the data shown in Figure 3. Virtually no change in transition temperature was observed with varied concentrations of MPD, as expected from the insensitivity of HPC thermodynamic force curves to added MPD (Figure 1). Measured and calculated slopes, $dT_c/d\Pi_s$, are given in Table 1.

waters associated with a 10 Å length of HPC, $\Delta\Gamma_w^{\text{total}}$, as the spacing between polymers is brought from a large separation to dryness ($D_{\text{Br}} = 10.9$ Å) are given in Table 1. There is a factor of about 3–4 difference between the most highly excluded solutes (α -methyl glucoside at 5 °C and KF) and the least (glycerol at 20 °C and KBr).

To facilitate comparison of these results with other measurements of exclusion, the distribution function can be approximated by a two-state model, a zone of complete exclusion and the bulk solution, by constructing an equivalent Gibbs dividing surface. A distance, ΔR , between the HPC and dividing surfaces can be defined such that if filled with pure water the number of waters within the volume would be $\Delta\Gamma_w^{\text{total}}$. These values are also shown in Table 1 for each solute and range from ~ 1 –4 Å. Essentially only the first hydration layer is affected by this criterion.

Effect of Salts on the Precipitation of HPC from Dilute Solution. The extracted spatial distributions of salt exclusion obtained with densely packed HPC arrays can be critically tested by independent measurement of the effect of salt on the reversible heat precipitation of HPC from dilute aqueous solution.¹⁸ Figure 4 shows the dependence of the cloud point temperature, T_c , on salt concentration for MPD, KF, KCl, and KBr. Consistent with the osmotic stress results, uniformly distributed MPD has no effect on precipitation. Excluded osmolytes favor precipitation since a release of excess water accompanies assembly. The slopes of these plots can be related to the changes in entropy and excess water associated with assembly by

$$\frac{dT_c}{dm_s} = \frac{d\Pi_s}{dm_s} \frac{kT\Delta\Gamma_w}{55.6\Delta S} \quad (10)$$

Osmotic pressures of the salt solutions are within 10% of their calculated van't Hoff values or $d\Pi_s/dm_s \sim 2$. The linear dependence of T_c on m_s suggests that both $\Delta\Gamma_w$ and ΔS are independent of osmolyte concentration. We have previously extracted changes in entropy as a function of Bragg spacing

from the temperature dependence of the thermodynamic force curves.¹⁸ Since the precipitation temperature from dilute solution (~ 41.5 °C) is nearly the same as temperature transition between repulsive and attractive forces measured in condensed arrays (~ 40.5 °C), we assume this entropy change adequately describes the precipitation from dilute solution. We can integrate plots of $\Pi_{\text{excess}}/\Pi_s$ vs D_{Br} to calculate $\Delta\Gamma_w$ using eq 7. The Bragg spacing between HPC macromolecules in the precipitated phase is ~ 12 Å. The results are summarized in Table 1. Experimental and calculated slopes are also shown for the neutral solutes. Consistent with their temperature-dependent exclusion, plots of T_c vs m_s for the neutral solutes are not linear (data not shown) for these osmolytes. Slopes for betaine glycine and α -methyl glucoside are estimated at 20 °C and compared to predicted slopes with $\Delta\Gamma_w$ calculated at 20 °C. The predicted slopes are within 10–20% of the observed values for the salts and for betaine glycine. There is more error for α -methyl glucoside. The entropy of exclusion for this sugar at the concentration necessary for precipitation at 20 °C, however, is comparable to the entropy of assembly itself.

Discussion

Through the sensitivity of intermolecular force curves to varying concentrations of salts and solutes, we have measured the interaction of several salts and solutes with the hydrophobically modified polymer hydroxypropyl cellulose. HPC is preferentially hydrated in the presence of the salts and polar osmolytes investigated. In contrast, there is no observable inclusion or exclusion of a nonpolar solute, MPD. The observed effect of salts on HPC force curves is consistent with classical Hofmeister behavior. Generally the anion species dominates Hofmeister effects. The ordering of anions seen here for the exclusion from nonpolar HPC, $F^- > Cl^- > Br^-$ is the same as for their exclusion from nonpolar benzene, for example, as measured by solubility.²⁷

Several aspects of the exclusion of salts and polar solutes that we observe here are characteristics commonly observed for the exclusion of solutes from proteins measured by densitometry and osmometry. A key empirical feature both of Hofmeister effects and of neutral osmolyte exclusion from surfaces that distinguishes these interactions from direct binding, is the approximate linear dependence of free energy perturbations on salt or solute concentration^{1–4,7,15} (and references therein). This linearity implies that preferential hydration coefficients, Γ_w , are independent of salt or solute concentration, i.e., the number of excess waters associated with the surface remains constant as the solute concentration is changed. Equivalently, a constant Γ_w implies that the partition coefficient of salt or solute is independent of concentration.

Courtenay et al.¹⁵ have further characterized the exclusion of several solutes from the protein BSA (bovine serum albumin) in terms of a two-state model. The most highly excluded solute, betaine glycine, acts as if there is no solute within about 3 Å of the protein surface (about a full hydration layer). Glycerol showed the weakest exclusion, with about 5-fold fewer included waters. The equivalent two-state approximations calculated here (Table 1) are within the same range of distances.

There are a great many macromolecular transitions and reactions that have now been shown sensitive to the presence of salts and osmolytes that are not direct participants in the conformational change or binding reaction. Once again, energy perturbations often vary linearly with solute osmotic pressure or concentration^{2,4,6–8} (and references therein) indicating a difference in the number of excess waters associated with the

products and reactants that is independent of solute concentration. HPC undergoes a precipitation transition as the temperature is increased. The transition temperature decreases with increasing concentrations of excluded salts and solutes since excess water is released as HPC polymers assemble. The calculation of the dependence of the precipitation temperature on salt or solute concentration or osmotic pressure shown in Figure 4 is a demanding test of the excess water distribution function we have extracted. The results summarized in Table 1 demonstrate that the slopes $dT_c/d\Pi_s$ are predicted quite well.

Exclusion of Salts and Solutes Consistent with a Repulsive Hydration Force. Several possible explanations for the exclusion of these salts and polar solutes are not consistent with these experiments on HPC. The electrical neutrality of HPC rules out electrostatics being central for understanding Hofmeister effects here. Nor does an electrostatic image-force model explain the data for neutral solutes whose distribution pattern is the same as salts.

The data cannot easily be explained by steric exclusion or "crowding". Steric exclusion from rough HPC surfaces could result in a change in Γ_w with spacing. A distribution of surface-to-surface distances and solute size could combine to give an apparent decay length. The difference in ionic crystal radii, however, would predict a greater exclusion of Cl^- (1.81 Å) than of F^- (1.33 Å). If ionic conductance is used as a measure of hydrated radius, then the difference in exclusion between Na^+ and K^+ salts should be as large as that observed between F^- and Cl^- , yet only differences between the anions are important. Furthermore, MPD that has a larger molecular volume than either glycerol or betaine glycine is not significantly excluded or included over the entire range of measured spacings. Nor is steric exclusion consistent with the temperature dependence of the neutral solutes.

The major advance of this work is the observation of the distance dependence that characterizes solute exclusion. The apparent exponential variation of $\Delta\Gamma_w$ with a 3–4 Å decay length seen for all the salts and solutes is strikingly similar to the repulsive forces measured between macromolecules at close spacing (the last 10–15 Å separation between surfaces) for many systems,¹⁷ ranging from charged and net neutral lipid bilayers^{28,29} to highly charged polymers (DNA^{21,24} and two stiff carbohydrates, xanthan,¹⁹ and *ι*-carrageenan), to completely uncharged polysaccharides (schizophyllan¹⁹ and HPC¹⁸). The forces between charged macromolecules exhibit only slight dependence on salt concentration at these close spacings, unlike their behavior at larger distances where electrostatic double layer forces clearly dominate. Indeed, contrary to general expectation the effect of salt on forces at these close spacings is far greater for neutral HPC than for highly charged DNA. These hydration forces have been measured between the neutral polymers schizophyllan and HPC across distilled water. The force between HPC polymers is temperature dependent showing increased entropy as surfaces approach, likely from the release of structured water from the condensed phase. We have suggested that the energetics of water structuring at close spacing between surfaces underlies the observed force.¹⁷ Within this framework, the magnitude of the hydration force depends on the mutual structuring of water on the two apposing surfaces. The 3–4 Å decay length reflects a water–water correlation length that has been observed for density fluctuations in liquid water.³⁰ There have been other formulations and measurements of the effects of water structuring on intermolecular forces, e.g.,^{10,31–33} (and references therein). Given the apparent strength and universality of hydration forces between macromolecules it is not surprising

that the distributions of these polar solutes and salts surrounding the nonpolar HPC polymer are also determined by water structuring interactions. Water structuring has long been thought to underlie Hofmeister effects of salts.^{1,9–11} A recent molecular dynamics simulation³⁴ of the interaction of the excluded osmolyte trimethylamine *N*-oxide (TMAO) with a small globular protein, chymotrypsin inhibitor 2, suggests that TMAO acts to stabilize the native conformation through solvent structuring.

The repulsive force between HPC polymers in water depends strongly on temperature.¹⁸ The repulsive force magnitude decreases as the temperature increases, changing from repulsive to attractive at ~40 °C. Given this strong temperature dependence, it is difficult to know which is more surprising—the temperature insensitivity of salt–HPC interactions or the temperature dependence of neutral solute–HPC exclusion. The preexponential factor of the repulsive force between HPC polymers in water decreases by almost a factor of 2 between 5 and 20 °C. We had speculated that the temperature sensitivity of HPC forces could result from temperature dependent differences in water structuring surrounding polar hydroxyl and nonpolar alkyl groups. This explanation can rationalize the temperature dependence seen for the exclusion for glycerol and α -methyl glucoside that are composed of the same chemical moieties and that also show an approximate 2-fold decrease in exclusion between 5 and 20 °C. It is also noteworthy that at both temperatures α -methyl glucoside is about twice as excluded as glycerol, suggesting that repulsive force magnitudes for homologous solutes scale with size. This size dependence would result if the total repulsive force magnitude were the sum of the individual contributions from constituent alkyl and hydroxyl groups.

Although the magnitude of exclusion for each salt is temperature insensitive, the decay length shows more variation than for the neutral solutes. There is a systematic increase from 2.9 Å for KBr to 3.8 Å for KCl to 4.5 Å for KF that accompanies increased exclusion. This variation could reflect the additional contribution from dispersion forces between ions and HPC.^{35,36} The polarizabilities of these ions differ greatly. The difference in decay lengths among the salts could also result from a difference in the exclusion of cations and anions from the HPC surface and a consequent charge separation. Both the hydration force decay length and the electrostatic Debye shielding length would then contribute to the spatial dependence of exclusion.

We have also recently investigated the exclusion of neutral solutes from highly charged DNA.²⁶ This system is almost the mirror image of HPC. Glycerol does not observably affect DNA forces and thus is neither included nor excluded. The nonpolar alcohols, 2-propanol and MPD, are strongly excluded from the highly charged DNA surface. Exclusion is again characterized by an exponential decrease in alcohol concentration as DNA surfaces approach with a 3–4 Å decay length. A repulsive hydration force also underlies the preferential hydration of DNA. Furthermore, MPD which is essentially two 2-propanol molecules joined together is excluded about 2-fold more strongly than 2-propanol, analogous to the 2-fold difference in exclusion from HPC between the homologous polyols glycerol and α -methyl glucoside that differ 2-fold in size. The exclusion of salts and solutes from surfaces mediated by water structuring interactions seems likely a general result. This observation represents a new viewpoint and suggests new tools to reexamine, systematize, and understand the vast, but generally phenomenological preferential hydration literature. The next important step would be a more systematic investigation of preferential

hydration and force measurements to connect the structure of water surrounding various chemical groups with their interaction energies.

Supporting Information Available: Text discussing and figures depicting the salt–PEG solution osmotic pressures and salt activities. This material is available free of charge via the Internet at <http://pubs.acs.org>.

References and Notes

- (1) Collins, K. D.; Washabaugh, M. W. *Q. Rev. Biophys.* **1985**, *18*, 323.
- (2) Davis-Searles, P. R.; Saunders, A. J.; Erie, D. A.; Winzor, D. J.; Pielak, G. J. *Annu. Rev. Biophys. Biomol. Struct.* **2001**, *30*, 271.
- (3) Eisenberg, H. *Biophys. Chem.* **1994**, *53*, 57.
- (4) Parsegian, V. A.; Rand, R. P.; Rau, D. C. Macromolecules and water: Probing with osmotic stress. In *Methods in Enzymology*; Johnson, M. L., Ackers, G. K., Eds.; Academic Press: New York, 1995; Vol. 259; p 43.
- (5) Parsegian, V. A.; Rand, R. P.; Rau, D. C. *Proc. Natl. Acad. Sci. U.S.A.* **2000**, *97*, 3987.
- (6) Record, M. T., Jr.; Zhang, W.; Anderson, C. F. *Adv. Protein Chem.* **1998**, *51*, 281.
- (7) Timasheff, S. N. *Annu. Rev. Biophys. Biomol. Struct.* **1993**, *22*, 67.
- (8) Timasheff, S. N. *Adv. Protein Chem.* **1998**, *51*, 355.
- (9) Hofmeister, F. *Naunyn-Schmiedeberg's Arch. Exp. Pathol. Pharmacol. (Leipzig)* **1888**, *24*, 247.
- (10) Cacace, M. G.; Landau, E. M.; Ramsden, J. J. *Q. Rev. Biophys.* **1997**, *30*, 241.
- (11) Leberman, R.; Soper, A. K. *Nature (London)* **1995**, *378*, 364.
- (12) Ellis, R. J. *Curr. Opin. Struct. Biol.* **2001**, *11*, 114.
- (13) Minton, A. P. *Curr. Opin. Struct. Biol.* **2000**, *10*, 34.
- (14) Schellman, J. A. *Biophys. Chem.* **1990**, *37*, 121.
- (15) Courtenay, E. S.; Capp, M. W.; Anderson, C. F.; Record, M. T., Jr. *Biochem.* **2000**, *39*, 4455.
- (16) Parsegian, V. A.; Rand, R. P.; Fuller, N. L.; Rau, D. C. Osmotic stress for the direct measurement of intermolecular forces. In *Methods in Enzymology*; Packer, L., Ed.; Academic Press: New York, 1986; Vol. 127; p 400.
- (17) Leikin, S.; Parsegian, V. A.; Rau, D. C.; Rand, R. P. *Annu. Rev. Phys. Chem.* **1993**, *44*, 369.
- (18) Bonnet-Gonnet, C.; Leikin, S.; Chi, S.; Rau, D. C.; Parsegian, V. A. *J. Phys. Chem. B* **2001**, *105*, 1877.
- (19) Rau, D. C.; Parsegian, V. A. *Science* **1990**, *249*, 1278.
- (20) Rau, D. C.; Parsegian, V. A. *Biophys. J.* **1992**, *61*, 246.
- (21) Strey, H. H.; Podgornik, R.; Rau, D. C.; Parsegian, V. A. *Curr. Opin. Struct. Biol.* **1998**, *8*, 309.
- (22) Cheng, Y.; Prud'homme, R. K.; Chik, J.; Rau, D. C. *Macromol.* **2002**, *35*, 10155.
- (23) Podgornik, R.; Rau, D. C.; Parsegian, V. A. *Macromol.* **1989**, *22*, 1780.
- (24) Podgornik, R.; Rau, D. C.; Parsegian, V. A. *Biophys. J.* **1994**, *66*, 962.
- (25) Leikin, S.; Rau, D. C.; Parsegian, V. A. *Phys. Rev. A* **1991**, *44*, 5272.
- (26) Hultgren, A.; Rau, D. C. *Biochem.* **2004**, *43*, 8272.
- (27) Long, F. A.; McDevit, W. F. *Chem. Rev.* **1952**, *51*, 119.
- (28) McIntosh, T. J. *Curr. Opin. Struct. Biol.* **2000**, *10*, 481.
- (29) Petrache, H.; Tristram-Nagle, S.; Gawrisch, K.; Harries, D.; Parsegian, V. A. *Biophys. J.* **2004**, *86*, 1574.
- (30) Xie, Y.; Ludwig, J. K. F.; Morales, G.; Hare, D. E.; Sorensen, C. M. *Phys. Rev. Lett.* **1993**, *71*, 2050.
- (31) Sorenson, J. M.; Hura, G.; Soper, A. K.; Pertsemliadis, A.; Head-Gordon, T. *J. Phys. Chem. B* **1999**, *103*, 5413.
- (32) Chalikian, T. V. *Annu. Rev. Biophys. Biomol. Struct.* **2003**, *32*, 207.
- (33) Chalikian, T. V. *J. Phys. Chem. B* **2001**, *105*, 12566.
- (34) Bennion, B. J.; Daggett, V. *Proc. Natl. Acad. Sci. U.S.A.* **2004**, *101*, 6433.
- (35) Bostrom, M.; Williams, D. R. M.; Ninham, B. W. *Langmuir* **2001**, *17*, 4475.
- (36) Bostrom, M.; Williams, D. R. M.; Ninham, B. W. *Biophys. J.* **2003**, *85*, 686.